



FORMATION OF POLYCRYSTALLINE STRUCTURE IN METALLIC FILMS IN THE EARLY STAGES OF ZONE I GROWTH

K. L. EKINCI and J. M. VALLES JR†

Department of Physics, Brown University, Providence, RI 02912, U.S.A.

(Received 9 September 1997; accepted 2 April 1998)

Abstract—The morphology of ultrathin Au and Pb films vapor deposited onto cryogenically cooled substrates has been studied by *in situ* Scanning Tunneling Microscopy (STM). At low substrate temperatures, $4 < T_S < 77$ K, where thermally activated grain growth processes are negligible, i.e. in the Zone I regime, films with equivalent bulk mass deposited thicknesses, $d \geq 0.9$ nm uniformly cover the substrate and exhibit no discernible crystalline structure for $d \leq 1.6$ nm for $T_S = 77$ K. Thicker films exist in a polycrystalline phase with a uniform grain size. It is argued that the observed polycrystalline structures do not form through normal thin film nucleation and growth processes. Instead, they form from a transient amorphous phase through athermal crystallization processes after a critical film thickness is reached. Results are also presented from annealing studies that support this view. © 1998 Acta Metallurgica Inc. Published by Elsevier Science Ltd. All rights reserved.

1. INTRODUCTION

The growth and structure of evaporated thin metal films has been the object of extensive investigation over the years. The importance of metal films in technological applications drives some of this work as does interest in the fundamental issues involved in the growth and the interplay between a film's physical properties and its structure. One of the primary factors determining the morphology of a film is the temperature of the substrate, T_S , during deposition. It is well established [1,2] that the average grain size in a wide range of films of different metals follows a nearly universal dependence on the ratio T_S/T_M , where T_M is the melting temperature of the metal. Four different growth zones have been identified corresponding to four qualitatively different film structures. At the highest temperatures, $T_S/T_M > 0.5$ (Zone III), thermally activated adatom diffusion, grain boundary motion and defect (e.g. dislocation) motion govern the grain growth and produce crystalline grains with dimensions roughly equal to the film thickness. These processes are relatively well understood [3,4]. In contrast, the processes governing the structure of films grown in the opposite extreme of very cold substrates remain unknown [1, 5–9]. These films, which have also been referred to as quench condensed, have been used in numerous studies of the effects of strong disorder on electronic transport [10]. Surprisingly, at tem-

peratures, $T_S/T_M < 0.1$ (Zone I), where thermally induced adatom diffusion, grain boundary motion and defect motion are negligible, X-ray diffraction and electron microscopy indicate that fine crystalline grains still manage to form for most metals with f.c.c. crystalline structure (e.g. Au, Cu, Ag, Pb). It has been speculated that the observed polycrystalline phases form from an amorphous phase through an athermal avalanche like process [1, 11].

In an effort to understand these low temperature growth processes, a series of *in situ* Scanning Tunneling Microscopy (STM) studies have been conducted of films of Au and Pb deposited on a variety of substrates held at 77 and 4 K, i.e. in the Zone I regime. These two f.c.c. metals have very different melting points which allows the investigation of films over a wide range of T_S/T_M (for Au $T_M = 1337$ K and for Pb $T_M = 601$ K). In a previous paper, observations of the structure of quench condensed Au films were reported [12]. In this report, measurements on quench condensed Pb films are described and compared with the results on Au films. The Au and Pb film morphologies exhibit a similar dependence on film thickness suggesting that the same grain formation process operates in the two cases. This result and the qualitative effects that annealing has on these films support the picture that crystalline grains in these films form from thin amorphous layers and the grain formation process is driven by the heat of crystallization. The grain crystalline orientations and shapes result from interfacial and surface energy minimization.

†To whom all correspondence should be addressed.

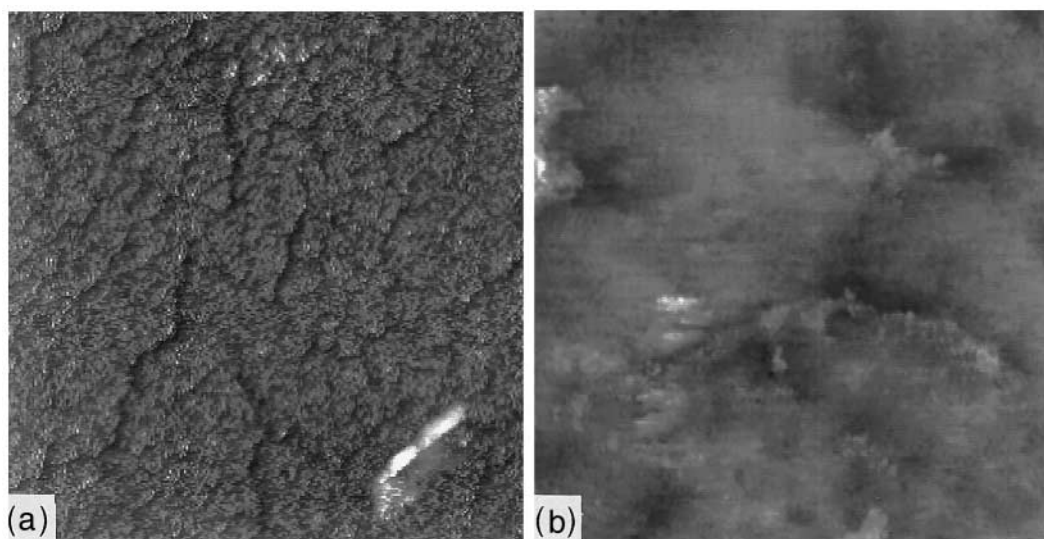


Fig. 1. *In situ* STM images of a 1.6 nm thick Au film deposited on a HOPG substrate held at 77 K. (a) The scan area is 1300 nm \times 1300 nm. The full scale height range from black to white is 2 nm. (b) A close up of the film shown in (a). The scan area is 170 nm \times 170 nm. The full scale height range from black to white is 1 nm.

2. EXPERIMENTAL TECHNIQUE

For measurements of the topography of films deposited onto substrates held at 4 and 77 K, a cryostat (described in detail elsewhere [13]) with thermal deposition and *in situ* STM probing capabilities was used. Briefly, the chamber containing the STM and thermal evaporation sources was cooled to cryogenic temperatures by direct immersion in liquid helium or nitrogen. Prior to immersion, a turbo pump evacuated the system to

$< 2 \times 10^{-7}$ Torr. During cool down, the change in the substrate temperature lagged the change in the temperature of the chamber walls, thus preventing the sample from cryo-pumping residual gases. The substrate remained at 300 K for approximately 1 h while the rest of the cryostat was at 77 K and at 77 K for approximately 2 h when the cryostat was at 4 K. The background pressure was estimated to be less than 1×10^{-8} Torr during 77 K depositions and 1×10^{-10} Torr during lower temperature depositions. To make films, high purity metals were thermally evaporated from a tungsten basket at a rate

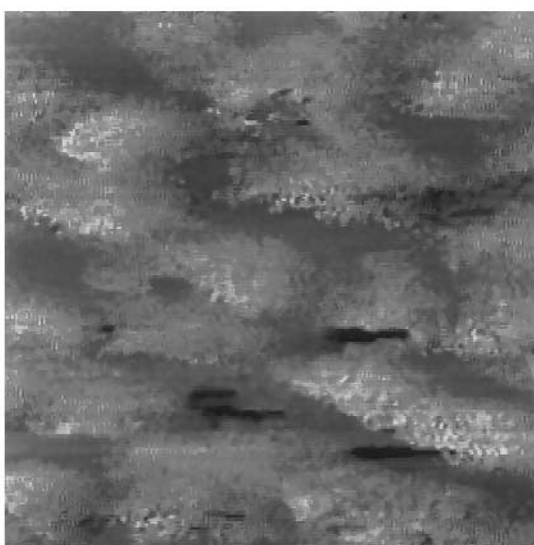


Fig. 2. *In situ* STM image of a 0.9 nm thick Pb film deposited on HOPG held at 77 K. The scan area is 220 nm \times 220 nm. The full scale height range from black to white is 1 nm.

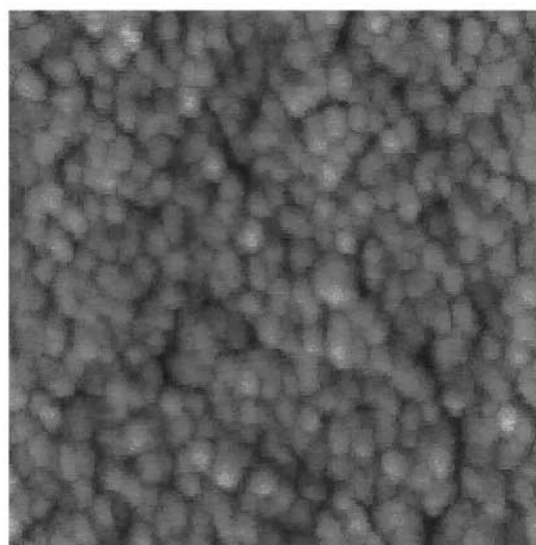


Fig. 3. *In situ* STM image of a 1.8 nm thick Au film on HOPG at 77 K. The scan area is 190 nm \times 195 nm. The height range of the grayscale is 1.5 nm.

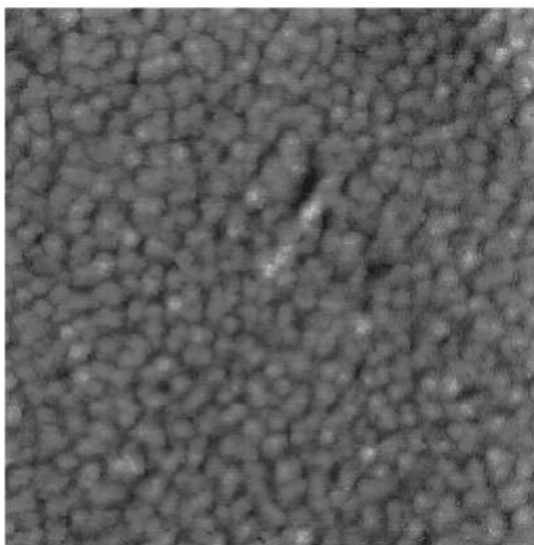


Fig. 4. *In situ* STM image of a 1.9 nm thick Pb film on HOPG at 77 K. The scan area is 372 nm \times 372 nm. The height range of the grayscale is 1.3 nm.

of 0.1–1 Å/s after being briefly outgassed behind a shutter. Film thicknesses and deposition rates were measured by a quartz crystal micro-balance. Substrate heating of approximately 5 K, as measured with a carbon resistance thermometer, was observed during Pb depositions on 4 K substrates. For Au depositions on 4 K substrates the heating was approximately 15 K. The substrate heating was negligible for the 77 K depositions.

A variety of substrates and substrate preparation techniques were employed to determine their influence on film growth and morphology. For 4 K depositions, Highly Oriented Pyrolytic Graphite (HOPG) was used as the substrate. For 77 K depositions HOPG, glass, amorphous Ge, and crystalline Au film substrates were employed. HOPG was used in the majority of the experiments on very thin films ($d < 1.0$ nm) due to its high electrical conductivity. The amorphous Ge substrates were prepared by *in situ* thermal deposition of three monolayers of Ge on a glass substrate held at 77 K, just prior to the film deposition. The crystalline Au substrates were prepared by depositing 20 nm of Au on HOPG held at 200°C while the rest of the cryostat was immersed in liquid nitrogen. This process created large crystalline structures with flat (111) faces with lateral dimensions greater than a few hundred nanometers. To test for the effects of substrate cleanliness on the obtained film structure, extensive substrate cleaning processes were employed (e.g. *in situ* cleaving of HOPG [14] or baking air cleaved HOPG [15] to 150°C for 2 h in the UHV conditions created by immersing the cryostat in liquid helium) for some of the experiments and the results were compared with experiments using less elaborate cleaning methods. To avoid contamination during

annealing studies, films were warmed to a set temperature and annealed for several hours while the cryostat was still in liquid nitrogen. Images of the annealed films were obtained after cooling them to 77 K.

STM measurements were made *in situ* in constant current mode at a bias voltage of 13–500 mV and a tunneling current of 0.5–10 nA.

3. RESULTS

3.1. Low temperature measurements

STM topographs show that the morphology of ultrathin Au and Pb deposits on various substrates at 4 and 77 K depends strongly on film thickness. At 77 K, films as thin as $d = 0.9$ nm deposited on UHV baked HOPG substrates, uniformly cover the flat regions of the substrate. It is noted that after such substrate cleaning processes, similar depositions at higher substrate temperatures ($T_S \cong 300$ K) result in the formation of large crystallites that nucleate at substrate defect sites such as step edges (results not shown). This observation showed the cleaning processes were effective for purging impurities from the HOPG surface. Figure 1(a) shows a large area topograph of a $d = 1.6$ nm Au film deposited on HOPG at 77 K. The substrate is uniformly covered and the film has an irregular texture that includes channel like structures that in some cases extend to the substrate. Figure 1(b) and Fig. 2 are smaller scans in Au ($d = 1.6$ nm) and Pb ($d = 0.9$ nm) films. In the Pb films, the channels appear more pronounced. The irregular topography and the fact that no discernible features smaller than 100 nm that could be associated with grains are present, hint that these films might be amorphous. Observations on thicker films support this view (see discussion below).

Slightly thicker films for both Au and Pb, exist in a granular phase. Figure 3 (Au) and Fig. 4 (Pb) are topographs of the thinnest films deposited on 77 K substrates that exhibited such a structure. In both experiments, the substrate (HOPG) was baked at 150°C in UHV conditions prior to the deposition. Both the Au film ($d = 1.8$ nm) and the Pb film ($d = 1.9$ nm) are composed of a single layer of closely spaced grains with clear gaps between some of them. In some places the gaps extend to the HOPG substrate. The grain height ranges between $1.0 < h < 1.8$ nm in Au films and $1 < h < 2.5$ nm in Pb films. The grains appear uniform in size, however grain size measurements are not completely trusted in single layer coverages since the finite size and shape of the tip might be of relevance for the resolution for such small structures in close juxtaposition [16].

Thicker films, such as those shown in Fig. 5(a) (Au) and Fig. 6 (Pb), exhibit a nonuniform height profile consistent with a layer by layer growth of

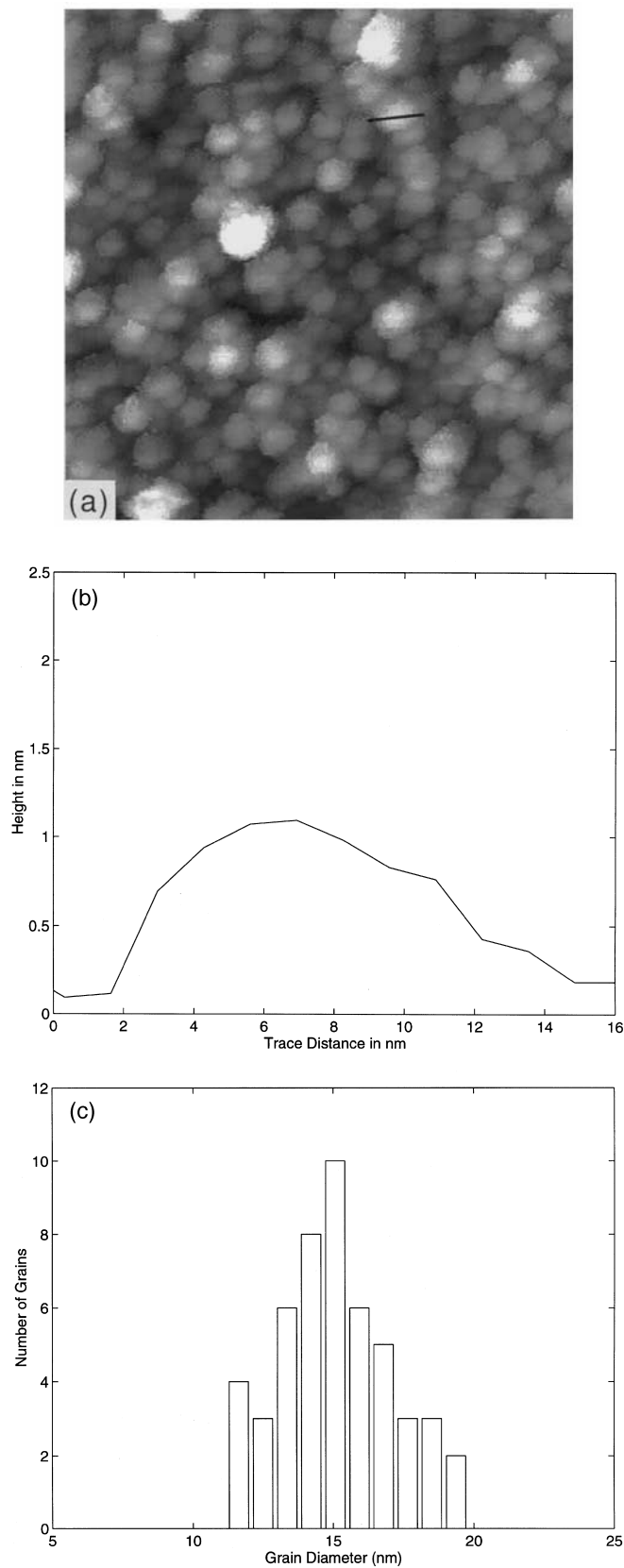


Fig. 5. (a) *In situ* STM image of a 2.2 nm thick Au film deposited on HOPG held at 4 K. The scan area is 145 nm \times 145 nm. The height range of the grayscale is 2.5 nm. (b) Line scan through the marked grain in (a). (c) Histogram of lateral grain dimensions of unobscured grains in (a).

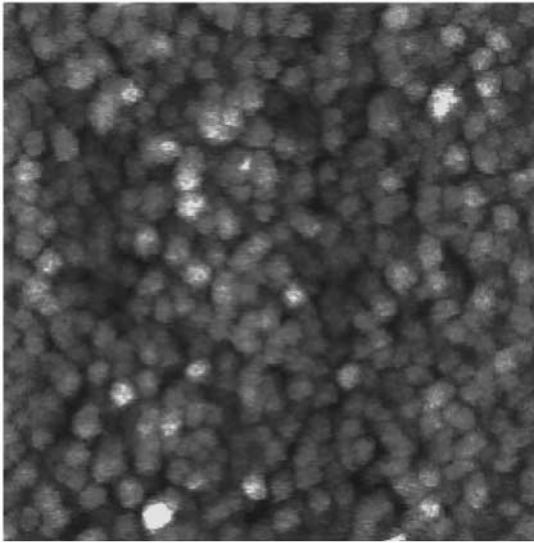


Fig. 6. *In situ* STM image of a 4.3 nm thick Pb film deposited on HOPG substrate held at 4 K. The scan area is $366 \text{ nm} \times 366 \text{ nm}$. The full scale height range from black to white is 6 nm.

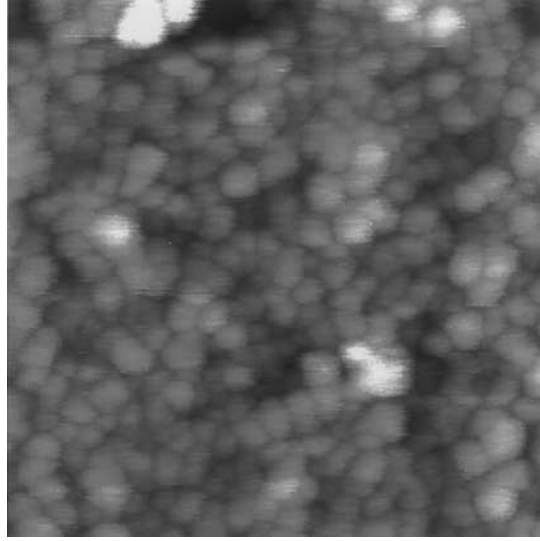


Fig. 7. *In situ* STM image of a 3.1 nm thick Au film deposited on amorphous Ge substrate. Three monolayers of Ge were deposited on a glass substrate held at 77 K just prior to the Au film deposition. The scan range is $178 \text{ nm} \times 179 \text{ nm}$. The full scale height is 5 nm from black to white.

the grains. The upper, unobscured grains are usually 1–2 nm above their neighbors, which allows measurements to be made of the grain shapes and sizes that are much less influenced by the tip geometry. A line trace [Fig. 5(b)] through an unobscured grain in Fig. 5(a) shows that the grain edges are rounded, and their tops are flat to one or two atomic layers over distances of $\sim 10 \text{ nm}$. The flat upper surfaces and regular shapes of the grains as well as the fact that it is possible to detect steps [Fig. 5(b)] that are approximately the size of atomic (111) steps in Au strongly suggest that these grains are crystalline. The histogram in Fig. 5(c) indicates that the grains have well-defined lateral dimensions, which are independent of the substrate temperature ($T_S \leq 77 \text{ K}$) during deposition (see Table 1).

Variations in substrate preparation and material did not seem to affect the morphology of the thicker films. Films deposited onto “clean” (UHV baked or *in situ* cleaved) or “dirty” (air cleaved) HOPG, fire polished glass, amorphous Ge (Fig. 7), crystalline Au films exhibit comparable grain sizes and aspect ratios.

3.2. Annealing studies

Annealing low temperature deposits of Au and Pb to room temperature produced different morphologies in the two cases. Warming (annealing)

the Au films with thicknesses, $2.1 < d < 10.0 \text{ nm}$, on HOPG to room temperature ($T/T_M = 0.22$) does not change the grain size but leads to the formation of cracks in the film. Figure 8 is a large area scan of an annealed Au film surface showing a typical areal density of cracks. The cracks come in a large range of sizes and shapes and do not show a preferred orientation. The fraction of the area covered by cracks ranges from 1% to as high as 20% of the total area of an image. The film surface at areas away from the cracks remains quite flat.

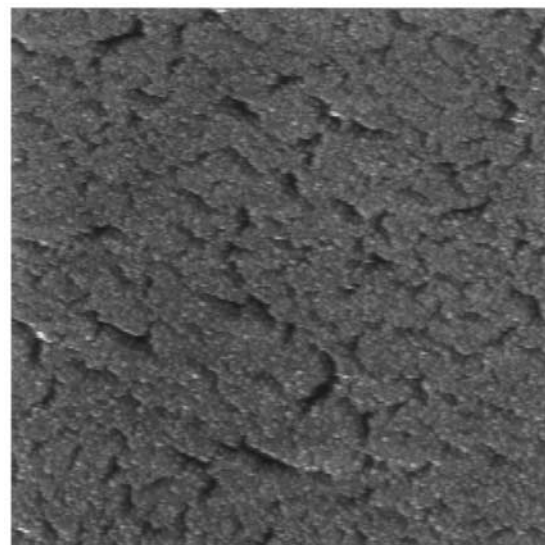


Fig. 8. STM image of a typical Au film ($d \cong 6 \text{ nm}$) on HOPG deposited at 77 K and annealed to room temperature. The scan area is $1200 \text{ nm} \times 1200 \text{ nm}$. The full scale height range is 5 nm.

Table 1.

Metal	Substrate temperature (K)	T_S/T_M	Grain diameter (nm)
Au	4	0.003	$11 < 2r < 20$
Au	77	0.058	$10 < 2r < 21$
Pb	4	0.007	$20 < 2r < 30$
Pb	77	0.128	$20 < 2r < 28$

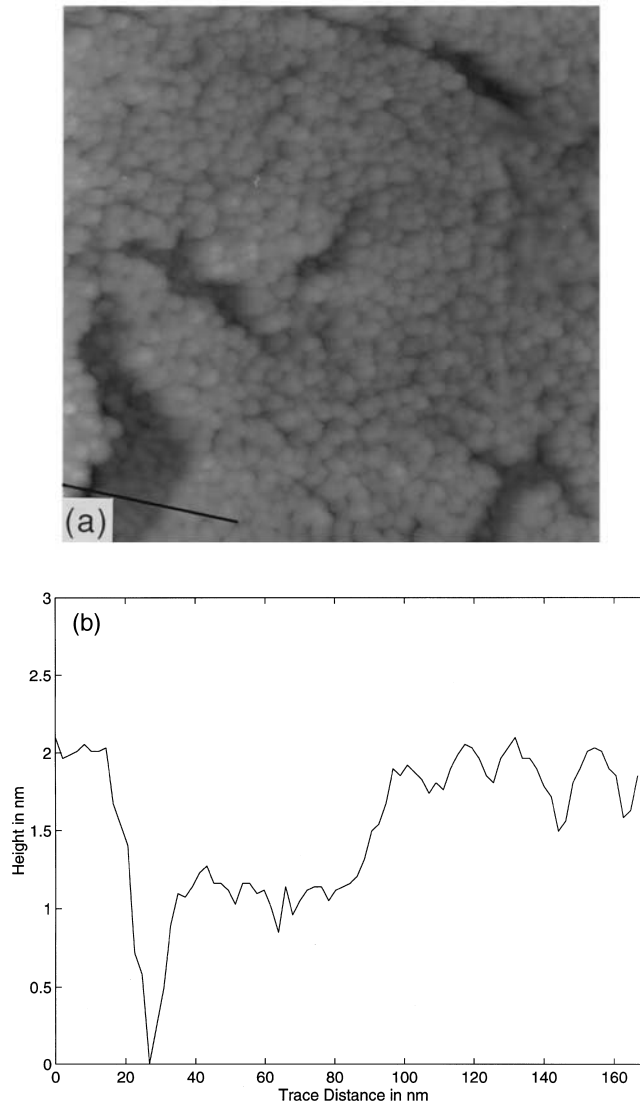


Fig. 9. (a) Close up of a cracked region in an annealed Au film ($d \cong 2.2$ nm) that was deposited on HOPG at 4 K. The scan area is $425 \text{ nm} \times 425 \text{ nm}$ and the height range is 2.5 nm. (b) Line scan through the cracked region showing the substrate and the two layers of grains.

Close inspection of some cracks reveals directly that grains grow upon grains. In the cracked region in Fig. 9(a) an underlayer of grains of size similar to the overlayer is visible. A line trace [Fig. 9(b)] through the large crack of Fig. 9(a) shows the presence of two layers of grains on the substrate (HOPG).

In contrast with the Au films, annealing to room temperature leads to extensive grain growth in the Pb films ($T/T_M = 0.50$ at room temperature) (Fig. 10). Similar grain growth is observed in Au films (Fig. 11), as the annealing temperature is raised further to 200°C ($T/T_M = 0.38$).

4. DISCUSSION

Although there have been many structural studies, the mechanisms involved in the formation of

structure in vapor deposited films in Zone I have not been elucidated. It is important to emphasize that normal thin film nucleation from the vapor phase and grain growth processes, as encountered in films grown in Zones II and III, cannot account for the formation of polycrystalline structures in Zone I [1,2]. In this section we discuss how observations provide insight into the factors governing grain formation in this low temperature regime. It is first useful to review some of the past work and contrast it with the present study of films grown in the Zone I thin film limit.

4.1. Earlier studies

Past electron microscopy and X-ray studies on Zone I films thicker than 50 nm have shown that they are composed of fine crystalline grains with nearly equal dimensions $5 < 2r < 20$ nm along all

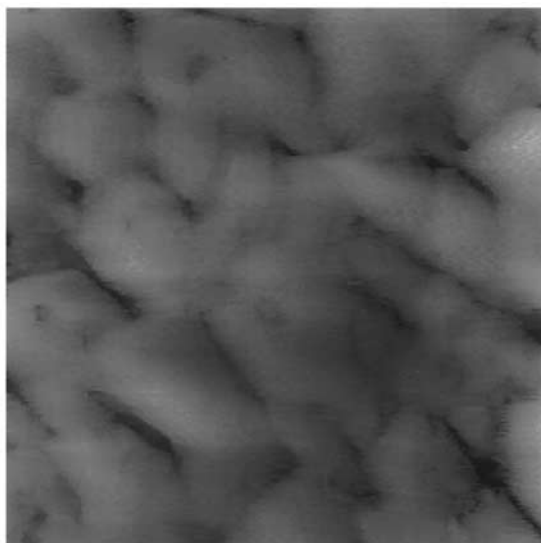


Fig. 10. STM topograph of a 6 nm thick Pb film deposited on HOPG held at 77 K after being annealed to room temperature. The scan area is 380 nm \times 380 nm and the height range is 6 nm.

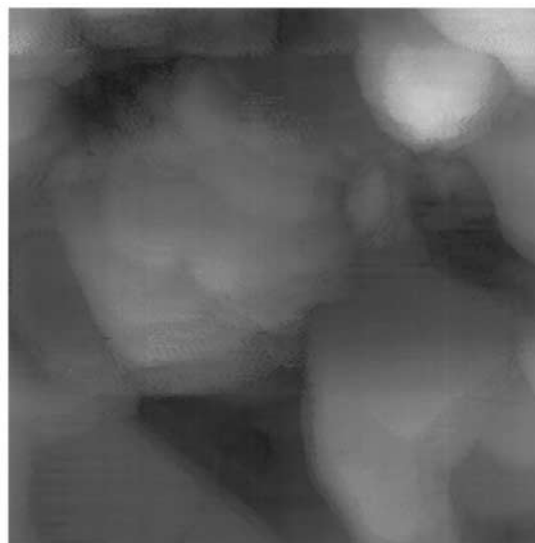


Fig. 11. STM topograph of a 6 nm Au film deposited at 77 K after being annealed to 200°C. The scan area is 917 nm \times 917 nm and the height range is 10 nm.

axes [1, 5–9]. In thin films, the grains seem to be oriented with their (111) planes parallel to the substrate and (100) texture is observed in thicker films [1, 8]. Annealing experiments [8, 9] also suggested that the grain size and orientation undergoes a change in the process of annealing to room temperature.

The fact that metal films deposited at low substrate temperatures have been observed in a polycrystalline phase is surprising, because normal crystalline nucleation and growth processes cannot account for the observed structures. Explicitly, an estimate for a crystallite size of ~ 10 nm and a monolayer per second deposition rate [2] shows that normal crystallite growth requires $T_s/T_M > 0.3$ for adatoms to be able to diffuse across the length of a typical terrace prior to colliding with atoms impinging from the vapor. For $T_s/T_M < 0.125$, the equilibrium diffusion constant is less than 10^{-15} cm²/s [2, 17]. It is also important to point out that impinging atoms thermalize with the substrate on time scales comparable to inverse phonon frequencies [18, 19]. This time is so short that the observed structures cannot form through diffusion of hot adatoms.

The above discussion suggests that in the extreme non-equilibrium limit of very low substrate temperatures, all metal films should form an amorphous phase. This argument accounts for the observed metastable, low density, amorphous phases in the low temperature deposits of semi-metals Bi and Sb [5, 20]. These films transform into the crystalline phase above a critical thickness or after annealing. It has been proposed [21, 22] that the stability of this metastable amorphous state is governed by the height of potential barriers hinder-

ing the motion of atoms to positions expected in an equilibrium crystal structure. In some metals, such as Bi, the amorphous state is fairly stable. For other metals like Au, Ag and Cu, however, such a metastable phase has not been observed previously even at very low substrate temperatures (~ 4 K).

It should be noted that the TEM and X-ray measurements were made on substantially thicker films (50–100 nm) than investigated in the present study. This limitation was imposed partially by the difficulties in obtaining diffraction patterns for ultrathin films (2–10 nm). Consequently, the thin film limit of growth phenomena was not studied in detail until the invention of a complimentary technique, the STM.

4.2. *In situ* STM studies

The *in situ* STM measurements on Au and Pb films deposited at cryogenic temperatures (Zone I) show that a film's structure depends strongly on its thickness in the ultrathin film limit. No crystalline structure is observable in films thinner than a critical thickness, d_c (at 77 K, $d_c \cong 1.7$ nm for Au and $d_c \cong 0.9$ nm for Pb), consistent with their being amorphous. Thicker films exist in a polycrystalline phase with a uniform grain size. The grains have a platelet shape with a large aspect ratio rather than being of equal extent in all directions. The height profile of the film becomes more nonuniform as the film thickness is increased and annealing studies in Au films reveal the existence of underlayers of grains. These results indicate that grains grow on grains. The fact that a similar structure has been observed for films deposited under a range of conditions at 4 and 77 K strongly suggests that a common athermal mechanism must govern their growth.

The observations that the grain size does not depend on T_S for $T_S < 77$ K in both Au and Pb films (see Table 1) and does not change upon annealing to 300 K in Au films, agree with the expectation that grain boundary motion is negligible at low substrate temperatures. The growth of Pb grains upon annealing to room temperature indicates that thermally activated grain boundary motion starts in the range $0.13 < T_S/T_M < 0.50$. The Au film annealing results constrains the range more tightly, suggesting that grain boundary motion starts in the range $0.22 < T_S/T_M < 0.38$. This range agrees with expectations based on the Zone Model of growth. The (111) orientation of the structures observed on crystalline and amorphous substrates indicate that the growth favors the minimization of interfacial and surface energies. In f.c.c. metals, the (111) planes have the lowest surface energy. Physically, the low surface energy of the (111) planes comes from the fact that they are the most densely packed planes [23]. These are the largest area surfaces on the crystallites in the present films.

The cracks in the Au films resulting from the annealing process to room temperature ($T/T_M = 0.22$ for Au) have too large an areal density to be accounted for by differential thermal contraction.† Consequently voids must exist between the grains of an as-deposited film. Thermal annealing drives the grains into a more efficient packing by filling these voids and in the process cracks form.

4.3. Growth model

A model of the growth of thin metal films on very cold substrates ($T_S/T_M < 0.1$) must describe an athermal process that produces platelet shaped grains with a uniform orientation and size distribution separated by voids. In addition, calculations of the height–height correlation functions‡ of images like Fig. 4, show that the surfaces are not correlated on length scales greater than a grain diameter. Hence, the athermal processes are believed to be local and random so that the structure in different regions of the film is uncorrelated. This mechanism contrasts with a long ranged mechanism that would select a certain wavelength [25].

The following mechanism is proposed for the growth. The deposited metal atoms initially “stick” where they land and form amorphous layers, such as those shown in Figs 1 and 2. Energy lowering interactions between the substrate surface and adatoms help stabilize the first few layers of the

amorphous film. However, as the film becomes thicker, the influence of the substrate wanes and the amorphous state transforms into the more stable polycrystalline state. The Au on Ge result (Fig. 7) supports this picture. Quench condensed Ge films have an amorphous structure to which the first Au atoms will be tightly bound. This strong interaction forces the Au to form an amorphous layer that is electrically continuous when very thin [26]. Making the Au deposit thicker (Fig. 7) leads to the formation of grains like those in Au on HOPG.

The thickness dependence of the onset of crystallization suggests that the crystallization process initiates at the upper free surface of the film. At these points, the energy cost to rearranging a few Au atoms into a crystalline cluster will be the least. The energy necessary for this process can come from a phonon, in the event that the barrier to rearrangement is small or, from the energy of a deposited atom, which is comparable to the binding energy. The energy of crystallization released provides the energy necessary for neighboring atoms to overcome the barrier holding them in the amorphous phase. Upon joining, these atoms release energy to others in the amorphous phase and the process continues. To sustain such an avalanche requires that the heat of crystallization exceed the barrier to moving an atom out of an “amorphous position” into a “crystal position”. This barrier is expected to be relatively small in f.c.c. metals like Au and Pb [21].

The grain orientations and shapes imply that interfacial and surface energy minimization governs the growth in the plane perpendicular to the plane of the film. As pointed out earlier, the (111) planes are the most densely packed and thus, this orientation minimizes the film substrate interaction energy. The in-plane growth is governed by the velocity of the resulting crystal to amorphous boundary and is expected to be proportional to its radius of curvature [27]. The upper limit on grain size might result from this driving force dropping below a critical value. In addition, since the onset of spontaneous crystallization can occur in random sites, growing crystals will impinge upon one another. The uniformity of the crystallite size distribution implies that relatively small grains can coalesce with larger grains and disappear and larger grains impinging on one another do not coalesce easily. The latter condition is reasonable as the energy barrier to coalescence grows with increasing grain radius. Since the amorphous phase is expected to be less dense than the crystalline phase, as the crystallites grow the vacancy density in the region around them increases since vacancies are driven away from the growing crystallite. Eventually, the density of atoms around the crystallite becomes sufficiently depressed to prevent further growth and voids form. These voids account for the presence of gaps

†The thermal expansion coefficients at room temperature for HOPG and Au are $20 \times 10^{-6}/^\circ\text{C}$ and $14.2 \times 10^{-6}/^\circ\text{C}$, respectively.

‡The height–height correlation function is defined as follows: if $h(\mathbf{x})$ is the height of the surface at position \mathbf{x} , $G(r) \equiv \langle [h(\mathbf{x}) - h(\mathbf{x} + \mathbf{r})]^2 \rangle$, where $\langle \rangle$ indicates an average over all vectors \mathbf{x} . For a detailed discussion see Ref. [24].

between grains in the thin granular films and the formation of cracks during thermal annealing.

The growth of similar layers of grains on top of the first layer on the graphite substrate implies that the above process repeats itself for each layer of grains. The first few layers of adatoms form an amorphous film on top of the preexisting crystallites and once the local thickness exceeds the critical thickness, a nucleus forms. This amorphous phase forms because the adatoms are unable to diffuse to equilibrium positions in the crystal face of a grain. Observations of uneven film profiles provide support for this aspect of the growth model. It is not expected to be able to resolve the featureless upper amorphous layer once crystallite structures have formed.

The mechanisms in this growth model may be active in determining film morphology at even higher substrate temperatures if other factors limit adatom motion during deposition. Films deposited on very dirty substrates in "poor" vacuum conditions [28] or films deposited very rapidly fall into this category. In the former case, adatom collisions with gas atoms or adsorbed species restricts their diffusion. In the latter case, adatoms are covered by the impinging layer prior to their diffusing any distance [1].

5. CONCLUSIONS

Detailed observations have been used of the structure of Au and Pb films deposited on a variety of substrates at cryogenic temperatures to propose a mechanism for film growth in the limit where thermally activated processes are negligible. Existing growth models, namely simple grain nucleation and growth are insufficient for explaining the formation of structure in these films. Observations suggest that athermal crystallization from an amorphous phase produces the morphology obtained.

Acknowledgements—Discussions with J. Kondev, T. Truscott, C. Elbaum and X. S. Ling are gratefully acknowledged. This study was supported by the NSF through DMR-9296192 and DMR-9502920.

REFERENCES

- Grovenor, C. R. M., Hentzell, H. T. G. and Smith, D. A., *Acta metall.*, 1984, **32**, 773.
- Ohring, M., *The Materials Science of Thin Films*. Academic Press, San Diego, 1991.
- Frost, H. J., Thompson, C. V. and Walton, D. T., *Acta metall. mater.*, 1990, **38**, 1455.
- Srolovitz, D. J., Anderson, M. P., Grest, G. S. and Sahni, P. S., *Scripta metall.*, 1983, **17**, 241.
- Buckel, W., *Z. Phys.*, 1954, **138**, 136.
- Mönch, W., *Z. Phys.*, 1961, **64**, 229.
- Bülow, H. and Buckel, W., *Z. Phys.*, 1956, **145**, 141.
- Vook, R. W. and Witt, F., *J. Vac. Sci. Technol.*, 1965, **2**, 49; Vook, R. W. and Witt, F., *J. Vac. Sci. Technol.*, 1965, **2**, 243.
- Yoshida, N., Oshima, O. and Fujita, F. E., *J. Phys. F: Metal Phys.*, 1972, **2**, 237.
- Dynes, R. C., Garno, J. P. and Rowell, J. M., *Phys. Rev. Lett.*, 1978, **40**, 479; Bergmann, G., *Phys. Rev. Lett.*, 1982, **48**, 1046; Strongin, M., Thompson, R. S., Kammerer, O. F. and Crow, J. E., *Phys. Rev. B*, 1971, **2**, 1078; Jaegar, H. M., Haviland, B. D., Goldmann, A. M. and Orr, B. G., *Phys. Rev. B*, 1986, **34**, 4920.
- Danilov, A. V., Kubatkin, S. E., Landau, I. L., Rinderer, L., *J. Low Temp. Phys.*, 1996, **103**, 1; Landau, I. L., Parshin, I. A. and Rinderer, L., *J. Low Temp. Phys.*, 1997, **108**, 305.
- Ekinci, K. L. and Valles Jr, J. M., *Phys. Rev. B*, in press.
- Ekinci, K. L. and Valles, J. M. Jr, *Rev. Sci. Instrum.*, 1997, **68**, 4152.
- Darby, T. P. and Wayman, C. M., *J. Cryst. Growth*, 1975, **28**, 41.
- Nishitani, R., Kasuya, A., Kubota, S. and Nishina, Y., *J. Vac. Sci. Technol. B*, 1991, **9**, 802.
- Gimzewski, J. K., Humbert, A., Bednorz, J. G. and Reihl, B., *Phys. Rev. Lett.*, 1985, **55**, 951.
- Gjostein, N. A., *Diffusion*. Am. Soc. Metals, Metals Park, Ohio, 1973.
- Tsymbalenko, V. L. and Shal'nikov, A. I., *Sov. Phys. JETP Lett.*, 1974, **18**, 329.
- McCarrol, B. and Enrich, G., *J. Chem. Phys.*, 1963, **38**, 523.
- Belevtsev, B. I., Komnik, Yu. F. and Yatsuk, L. A., *Sov. Phys. Solid St.*, 1973, **14**, 1887.
- Komnik, Y. F., *Sov. J. Low Temp. Phys.*, 1982, **8**, 1 and references therein.
- Kubatkin, S. E. and Landau, I. L., *Sov. Phys. JETP*, 1989, **69**, 420.
- Thompson, C. V., *A. Rev. Mater. Sci.*, 1990, **20**, 245.
- Krim, J. and Palasantzas, G., *Int. J. Mod. Phys. B*, 1995, **9**, 599.
- Srolovitz, D. J., *Acta metall.*, 1989, **37**, 621.
- Hsu, S.-Y. and Valles, J. M. Jr, *Phys. Rev. Lett.*, 1995, **74**, 2331.
- Thompson, C. V., *Mater. Res. Soc. Symp. Proc.*, 1994, **343**, 13.
- Ekinci, K. L. and Valles Jr, J. M., unpublished.